Seismic risk reduction of existing RC buildings retrofitted with steel braces

Redução do risco sísmico de edifícios existentes de betão armado reforçados com contraventamentos metálicos

Rodrigo Falcão Moreira
Romain Sousa
Humberto Varum
José Miguel Castro

Abstract

The purpose of this paper is to present a study which analyses the evolution of a building portfolio's seismic risk, between its original conditions and those created by duly designed strengthening interventions. A sample of artificially generated non-seismically designed RC buildings, retrofitted to fulfil the requirements of the applicable EC8-3 limit state, is used for that purpose. The required fragility functions are derived following an analytical methodology based on nonlinear static analyses and procedures, the recently developed ESRM20 exposure model for Portugal is adopted for the spatial distribution and economic value of the assets, and the open-source software *OpenQuake* is used to determine loss ratios per region and building class. The evolution of seismic risk is then analysed and discussed, comparing the results for the original buildings with those for their retrofitted counterparts.

Resumo

O presente artigo apresenta um estudo que analisa a evolução do risco sísmico de um portfolio de edifícios, entre as suas condições originais e aquelas criadas por intervenções de reforço devidamente dimensionadas. Para o efeito, é usada uma amostra artificialmente gerada de edifícios de betão armado não sismicamente dimensionados, os quais foram reforçados de forma a satisfazerem os requisitos do estado limite exigido pelo EC8-3. As necessárias funções de fragilidade são derivadas através de uma metodologia analítica baseada em análises e procedimentos não-lineares estáticos, o recentemente desenvolvido modelo de exposição ESRM20 para Portugal é adotado para definir a distribuição espacial e valor económico dos edifícios, e o software *OpenQuake* é utilizado para determinar rácios de perdas por região e classe de edifícios. A evolução do risco sísmico é depois analisada e discutida, comparando os resultados obtidos para os edifícios originais com aqueles dos edifícios reforçados.

Keywords: RC buildings / Seismic retrofitting / Risk analysis / Concentric steel braces / Displacement-based design

Palavras-chave: Edifícios de betão armado / Reforço sísmico / Análise de risco / / Contraventamentos metálicos concêntricos / / Dimensionamento baseado em deslocamentos

Rodrigo Falcão Moreira

Assistant Professor
CONSTRUCT-LESE
Porto, Portugal
rem@isep.ipp.pt

Romain Sousa

Researcher
RISCO, UA
Aveiro, Portugal
romain.sousa@gmail.com

Humberto Varum

Full Professor
CONSTRUCT-LESE
Porto, Portugal
hvarum@fe.up.pt

José Miguel Castro

Associate Professor
CONSTRUCT-LESE
Porto, Portugal
miguel.castro@fe.up.pt

FALCÃO MOREIRA, R. [*et al*.] – Seismic risk reduction of existing RC buildings retrofitted with steel braces. **Revista Portuguesa de Engenharia de Estruturas**. Ed. LNEC. Série III. n.º 22. ISSN 2183-8488. (julho 2023) 55-66.

1 Introduction

The effectiveness of steel-brace retrofitting systems designed to strengthen existing RC buildings can be demonstrated by evaluating the performance of the retrofitted structures according to the requirements of Part 3 of Eurocode 8 (EC8-3). However, to analyse the evolution of a building portfolio's seismic risk, between its original conditions and those created by the strengthening interventions, it is necessary to go beyond the verification of code criteria compliance. Fragility functions are required, as well as an exposure model that defines the spatial distribution and economic value of the building typologies under analysis, both of which must then be combined with a seismic hazard model deemed adequate for the locations under analysis. The purpose of this paper is to present such a study.

Fragility functions provide the probability of exceeding a set of damage states as function of a ground motion intensity measure (usually ground or building response) and have been recognized in the last decades as a fundamental tool to assess seismic risk. When combined with a consequence model that relates each damage state with a loss ratio (i.e., the ratio of absolute economic loss to total replacement cost), they generate vulnerability functions, which provide the probabilistic distribution of loss ratio as function of the same intensity measure. Empirical methodologies, based on observed building damage and repair cost data from past earthquakes, have been traditionally used to produce such functions. However, several studies (e.g., [1]) propose the use of analytical methodologies as a way to overcome limitations such as the frequent lack of post-earthquake data. To evaluate how the capacity, fragility, vulnerability, and risk outputs are influenced by these methodologies, Silva *et al.* [2] conducted a study comparing static and dynamic approaches and discussed the relative accuracy between them. The results of that study showed similarity between the vulnerability functions obtained through a displacement-based adaptive pushover (DAP) analysis, combined with the N2 method, and those obtained through nonlinear dynamic analysis. This conclusion suggests that nonlinear static procedures may be a valid alternative for the rapid and accurate assessment of seismic vulnerability, which is quite an important finding for large-scale studies. More details can be found in the original research paper, to which readers are strongly referred to.

The fragility functions used herein are therefore derived following an analytical methodology based on nonlinear static analyses and procedures. The assessment of seismic risk is then performed using the open-source software *OpenQuake* [3]. The obtained loss ratios are compared, and the effects of the retrofitting systems analysed and discussed. The detailed framework of the conducted study is presented below. Readers should, however, be aware that no building-to-building variability (i.e., variability of material and geometrical properties within the defined sample) was considered simply because the retrofitting design procedure that was used is not yet fully automatized [4], making it thus impracticable to swiftly retrofit what would become a much larger sample of pre-code RC buildings obtained through Monte Carlo simulation. Although the authors recognize that this option may be seen as a limitation of the devised strategy, they also believe it does not compromise the above-referred purpose of the performed study, therefore can be accepted without prejudice.

2 Framework of the study

The considered sample of buildings includes ten non-seismically designed RC buildings, plus two sets of ten correlated retrofitted buildings designed to withstand the seismic demand defined by two hazard scenarios (S3 and S4, characterized in Table 1). Buildings with 2, 3, 4, 5, and 6 storeys were generated, with two regular plans (3 × 5 and 2 × 4 spans), to be analysed in separate directions (henceforth referred to as XX and YY). As an example, figures 1 and 2 show images of the nonlinear analysis models developed for two of the buildings, and of the retrofitting system designed for another (full details can be found in [4]). Six building classes were considered within the sample: concerning the number of storeys, the classification proposed by Silva [5] is followed, i.e., buildings up to three storeys are low-rise (LR), and those between four and six storeys are mid-rise (MR); concerning the structural design approach, original buildings are termed "PC", while their retrofitted counterparts are termed "R1" and "R2". This allows results – in terms of structural fragility and seismic risk – to be organized in a way that enables the desired view over the evolution between the original conditions and those created by the strengthening interventions.

The process of deriving the required fragility functions starts with the generation of capacity curves for the original and retrofitted structures, originating a total of sixty curves (twenty for the original structures, and forty for the retrofitted structures). Each curve is transformed into that of the equivalent SDOF system, and a nonlinear static procedure is used to estimate the target displacements for a selected set of ground motion records. These estimates are then compared with limit state (LS) displacements to determine, within

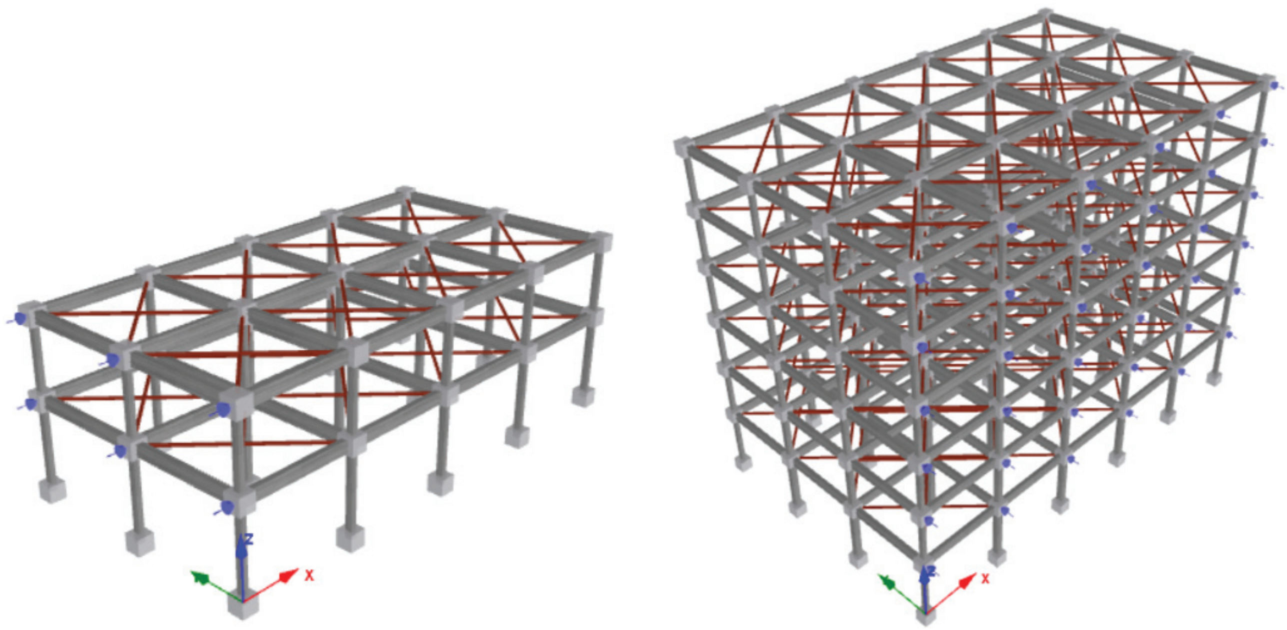

(i) (ii)

Figure 1 Numerical models for two of the original RC buildings: (i) 2S_2 × 4_XX; (ii) 6S_3 × 5_YY

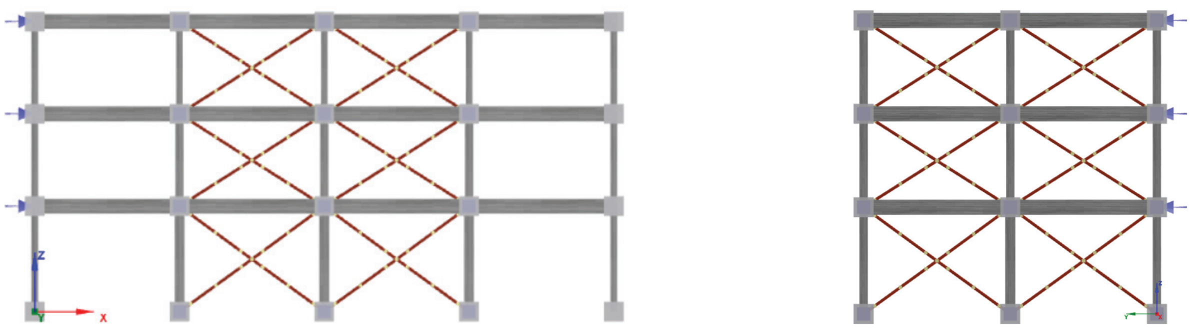

Direction XX Direction YY

Figure 2 Example of the proposed retrofitting systems (concentric X-diagonal steel braces composed by hot-rolled circular hollow section profiles): S4_3S_2 × 4_RETRO each building class and per ground motion record, the number of structures in each damage state. In order to graphically represent these results, an intensity measure of the imposed seismic demand (i.e., of the selected ground motion records) must be chosen. From the available options, the spectral acceleration at the fundamental vibration period $S_a(T_1)$ has been advocated by many authors (e.g., Bommer *et al.* [6]), as it provides good correlation with building damage. It also seemed like the best option for the purpose of this study. However, as each sampled structure has its own fundamental vibration period T_1, the mean value of the latter is considered across each building class. Scatter plots are thus generated (one per building class), relating the spectral acceleration $S_a(T_1)$ of each ground motion record with the respective number (in percentage) of structures that fail under its action. Finally, using least squares regression to fit a lognormal cumulative distribution to the data, the fragility functions are derived.

Table 1 Seismic hazard scenarios for the assessment and retrofitting process

Scenario	Hazard level	EC8-1 seismic zone	Region of Portugal
S3	Moderate	1.3	Lisbon
S4	High	1.1	West Algarve

The seismic risk assessment process is then carried out, starting with the definition of the input components required by the *OpenQuake* engine: (i) the seismic hazard model; (ii) the exposure model; (iii) the vulnerability model. For the hazard model, the seismic ruptures' characteristics are based on the work of Carvalho *et al.* [7], the ground motion fields are estimated with the ground motion prediction equations (GMPE) proposed by Atkinson and Boore [8] and Akkar and Bommer [9], and the amplification effects due to the local site conditions are handled through the approach described in [3]. For the spatial distribution of the assets and economic value of their structural components, the ESRM20 exposure model for Portugal (included in the recently developed European Seismic Risk Model (ESRM20) [10]) is adopted. As for the structural vulnerability model, the corresponding functions are obtained combining the derived fragility functions with an adequate consequence model (as previously referred). These three components are provided as input to the *OpenQuake* scenario risk calculator, which provides the above-referred loss ratios, per region and building class. Finally, the evolution of seismic risk is analysed comparing the results for the original buildings with those for their retrofitted counterparts. The following sections provide further details on the performed fragility and risk analyses.

3 Fragility analysis

3.1 Selection of ground motion records

Several ground motion record selection techniques have been proposed in the last years, ranging from simple procedures based on magnitude, distance, and site conditions, to more complex procedures that consider the spectral shape for each site, the hazard level, and the structural vibration period(s) of interest [11]. In the current study, the recent recommendations by Araújo *et al.* [12] were followed. For each of the site locations corresponding to the above-referred hazard scenarios S3 and S4, a set of forty ground motion records was selected and scaled to obtain proper matching between the set's mean spectrum and the EC8-1 elastic response spectrum. The process was conducted using the SelEQ tool [13]. Figure 3 shows the individual, median, and mean spectra of the two sets of records, as well as the target response spectrum for each.

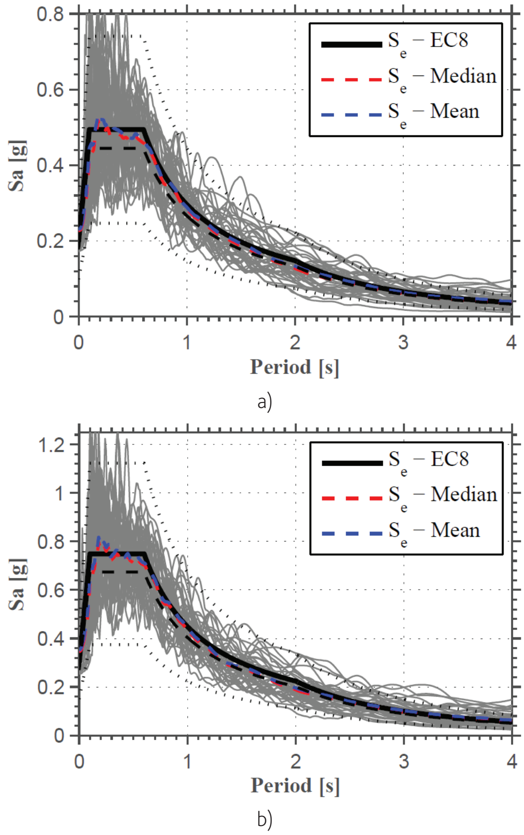

Figure 3 Response spectra of the selected ground motion records and corresponding EC8-1 target spectrum (475-yrp; ξ_0 = 5%; type B ground): a) Lisbon (1.3); b) West Algarve (1.1)

The selected ground motion records were obtained from real earthquake events. The seismological criteria for the preliminary search that is first carried out by SelEQ were based on the characteristics of the events that define zones 1.3 and 1.1 of the Portuguese territory, according to the country's National Annex (NA) in EC8-1. Magnitudes and epicentral distances higher than 5.5 and 20 km, respectively, were considered accordingly. Additionally, an interval of values between 360 m/s and 800 m/s was considered for the average shear wave velocity $v_{s,30}$, in agreement with the type B ground as defined in EC8-1. The preliminary search results were then narrowed down by imposing spectral compatibility between the mean spectrum of the group and each target response spectrum, within the period intervals defined in EC8-1. In the optimization process, the scaling factors were limited to the interval between 0.5 and 2.0, the mismatch between the mean spectrum of the group and each target spectrum was limited to an interval of ± 10%, and the mismatch between each individual record and each target spectrum was limited to an interval of ± 50%. This process led to the above-referred two sets of forty records.

3.2 Definition of limit states

As discussed in [14], there are several options for the engineering demand parameters (EDP) that can be used to allocate buildings to a damage state. These include the maximum roof displacement, inter-storey drift ratio, steel or concrete strain levels, base shear, etc. Each option will naturally lead to different damage distributions, hence different fragility functions. This dependence has been the object of several studies (e.g., [15]), to which readers are referred to, but will not be further addressed herein. Damage states, which may be associated with both structural and non-structural components, represent growing levels of installed damage (e.g., none; slight; moderate; extensive; collapse) due to the seismic demand. The transition from a given damage state to the next implies incurring the limit state (LS) separating them, i.e., reaching the adopted EDP's threshold that represents that particular LS. The definition of EDP thresholds corresponding to growing levels of damage has also been the object of several studies. For instance, Ghobarah [16] and Sassun *et al.* [17] proposed inter-storey drift ratio limits for different structural systems. These recommendations can be taken as reference. However, for structural systems outside the scope of these proposals, alternatives must be found. Such was the case of a recent study [18] concerning the derivation of fragility functions for Portuguese RC precast buildings.

Given the purpose of this study, and to maintain coherence with the performance requirements adopted for the seismic assessment, the same structural LS – Significant Damage (SD) – was considered herein to derive the required fragility functions. According to EC8-3, it is characterized as follows: "The structure is significantly damaged, with some residual lateral strength and stiffness; vertical elements are capable of sustaining vertical loads; non-structural components are damaged, although partitions and infills have not failed out-of-plane; moderate permanent drifts are present; the structure can sustain after-shocks of moderate intensity; the structure is likely to be uneconomic to repair." As referred in [4], the failure mechanism of the generated buildings' critical columns at the LS of SD is governed by their shear force capacity. Hence, the inter-storey drift limits used herein to define the LS were those which cause the critical columns' shear demand to come close to the corresponding capacity – which are in fact the same that guided the design of the retrofitting systems (full details can be found in [4]). They range between 0.50% and 0.65%, which compares well with the interval proposed in [16] for an equivalent damage state of non-ductile RC frames (0.50 % to 0.80%).

3.3 Fragility functions

As previously referred, the fragility functions were derived using the capacity curves of the original (PC) and retrofitted (R1 and R2) structures and the N2 method to estimate the target displacements for each of the selected ground motion records. The latter were scaled seven times to ensure the full coverage of the capacity curves, leading to 16 800 target displacements per each set of ground motion records (60 curves × 40 records × 7 scale factors). The results were then compared with the above-defined LS displacements (duly transformed into those of the equivalent SDOF systems) to determine, within each of the defined building classes and per ground motion record, the percentage of structures that incurred the LS of SD. Scatter plots relating these percentages with the spectral acceleration S_a (T_1) of each ground motion record were created, and a lognormal cumulative distribution was then fitted to the data using least squares regression, providing one fragility function per building class for each set of ground motion records. Both the capacity curves and the scatter plots can be found in [4]. The statistical parameters of the adjusted lognormal distributions are given in Table 2. Concerning the correlation between the curves and the individual data, this was found to be quite acceptable, as the calculated correlation values r^2 are equal or higher than 0.85 on all curves. Figures 4 and 5 compare the before and after retrofitting fragility functions, separated according to building class in terms of number of storeys (LR or MR) and to selected ground motion records set (S3 or S4), as to analyse the changes that occur in the probability of exceeding the LS of SD after the designed retrofitting systems (R1 or R2) are added to the original structures.

Table 2 Statistical parameters of the fragility functions (in terms of spectral accelerations at elastic period T_1)

Building classes		GM records set S3		GM records set S4	
		λ (m/s²)	ζ (m/s²)	λ (m/s²)	ζ (m/s²)
PC	LR	0.68	0.17	0.66	0.39
	MR	0.84	0.34	0.93	0.29
R1	LR	1.32	0.24	1.29	0.25
	MR	1.27	0.23	1.24	0.29
R2	LR	1.86	0.26	1.91	0.23
	MR	1.83	0.20	1.84	0.18

Statistical parameters: λ = logarithmic mean; ζ = logarithmic standard deviation

The above-presented comparisons show that, for the same value of spectral acceleration *Sa* (T_1), the curves for the retrofitted structures always return lower probabilities of exceedance than those for the original structures. Moreover, if one considers the EC8-3 (2005) values of S_a (T_1) for each building class (i.e., those obtained from the response acceleration spectra for the LS of SD), the probabilities of exceedance for the original structures are quite high, while those for the retrofitted structures stay below 50%. As such, the obtained results confirm the designed retrofitting systems' ability to effectively improve the seismic capacity of the analysed pre-code RC structures and contribute to the reduction of the seismic risk to which such buildings may be exposed. Concerning the effect of the

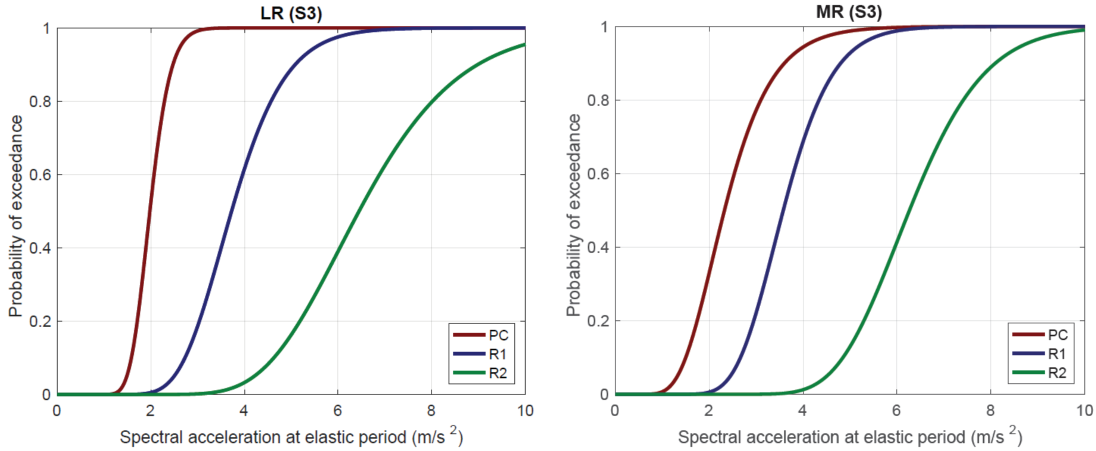

a) b)

Figure 4 Comparison of structural fragility functions for the LS of SD, derived using the ground motion records selected for the Lisbon region (scenario S3), between original and retrofitted buildings: a) Low-rise; b) Mid-rise

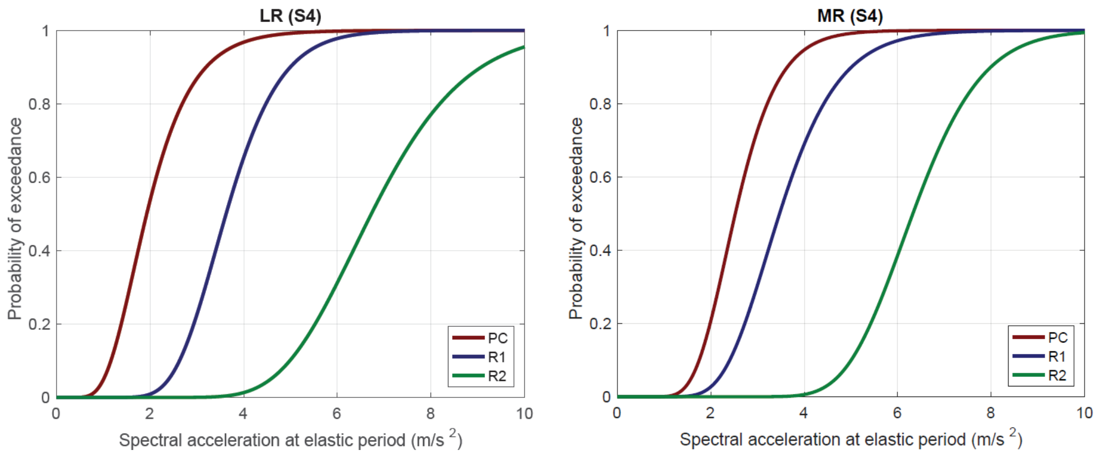

a) b)

Figure 5 Comparison of structural fragility functions for the LS of SD, derived using the ground motion records selected for the West Algarve region (scenario S4), between original and retrofitted buildings: (a) Low-rise; (b) Mid-rise

number of storeys, the comparison between fragility functions for the LR and MR retrofitted buildings shows no significant differences. The graphical similarity between curves is (naturally) confirmed by the statistical parameters λ and ζ given in Table 2. The fact that the structural fragility of the retrofitted buildings is not significantly affected by the increasing number of storeys is an encouraging finding, as it further goes to show the ability of steel-braced retrofitting systems to stabilize the lateral behaviour of pre-code RC structures. However, given the limited size of the sample considered in this study, neither generalized conclusions should be drawn, nor should these fragility functions be used for purposes other than those defined within the scope of this study. Lastly, concerning the effect of the selected ground motion records set (S3 or S4) on the fragility functions, the similarity between those obtained for each is also noticeable. However, this similarity is not surprising, as the target spectra for both record sets have the same shape, with different peak ground accelerations, thus inevitably leading to similar selections of ground motion records, except for the scale factors. As such and given the considerable number of records in each set, no relevant differences were in fact expected between the two sets of fragility functions.

4 Risk analysis

4.1 Hazard model

In terms of plate tectonics, Portugal is located at the southwest part of the Eurasian plate, near where the African and North American plates meet. Consequently, it may experience offshore seismic events with large to very large magnitude, and onshore events with moderate to large magnitude [19]. Two different earthquake scenarios, representing the country's most relevant seismic sources, were therefore considered in this study for the assessment of potential structural losses: (i) a strong magnitude offshore event, associated with an inter-plate rupture at the Eurasian-African interface; (ii) a moderate onshore event, associated with an intra-plate rupture at the Tagus Valley fault. The assumed parameters for these two ruptures were based on the work of Carvalho *et al.* [7] and are summarized in Table 3. The surface projections of the hypothesised faults are shown in Figure 6, adapted from the work of Silva *et al.* [20] which considered the same two seismic events.

Table 3 Assumed source parameters for the considered earthquake scenarios

Rupture	Magnitude (M_w)	Center of fault	Strike	Dip	Rake
Offshore	7.6	36.90 N; 9.90 W	20°	24°	90°
Onshore	5.7	38.82 N; 9.05 W	220°	55°	0°

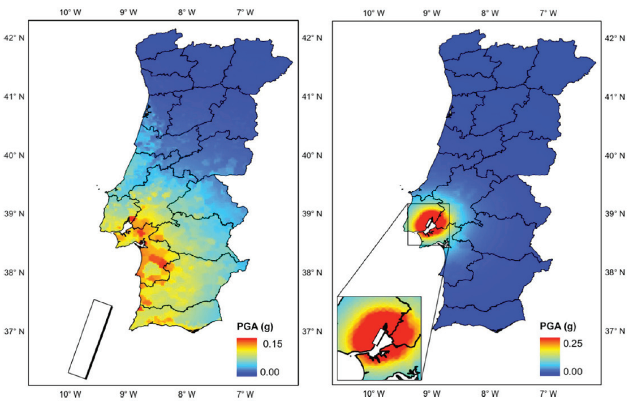

a) b)

Figure 6 Median ground motion fields for the offshore a) and onshore b) events (ad. [20])

The ground motion fields for the offshore event were calculated using the GMPE proposed by Akkar and Bommer [9], while those for the onshore event were obtained with the GMPE proposed by Atkinson and Boore [8]. The former are one of the most popular proposals for shallow crustal earthquakes in Europe, while the latter are known to perform reasonably well for close-distance events in mainland Portugal. The selection of an adequate attenuation model for Portugal is challenging due to the lack of ground motion recordings to support the development of specific GMPE or, at least, enable a reliable verification of existing models. However, recommendations on this topic can be found in [21] and [22]. As for the influence of site conditions, the average velocity of seismic shear waves in the top 30 meters layer ($v_{s,30}$) was used to characterize it, following the approach described in [3]. One-thousand ground motion fields were generated for each earthquake scenario using the *OpenQuake* engine, thus duly ensuring the propagation of the models' aleatory uncertainty through the loss assessment results. The spatial distribution of the median peak ground acceleration (PGA) is depicted in Figure 6.

4.2 Exposure model

The recently developed ESRM20 exposure model for Portugal (see [10]) was adopted in this study to define the spatial distribution and economic value of the assets. According to it, there is a total of 3 353 762 residential (RES) buildings in the mainland territory, adding up to a total replacement cost of 504 074 M€. The number of RC buildings is equal to 1 599 434 (about 47.7% of the total), from which 627 151 were erected before the publication of the RSA design code [23] and can thus be categorized as pre-code (PC). Within the latter, 573 779 are categorized as low-rise (LR), and 43 973 as mid-rise (MR). In terms of spatial distribution, a significant percentage of the RES buildings on the mainland are located in the Porto, Aveiro, Lisbon, and Setubal districts – for instance, for the RC-PC-LR and -MR building classes, respectively 42.9% and 78.3%. The distribution of the assets included in those two building classes is shown in Figure 7.

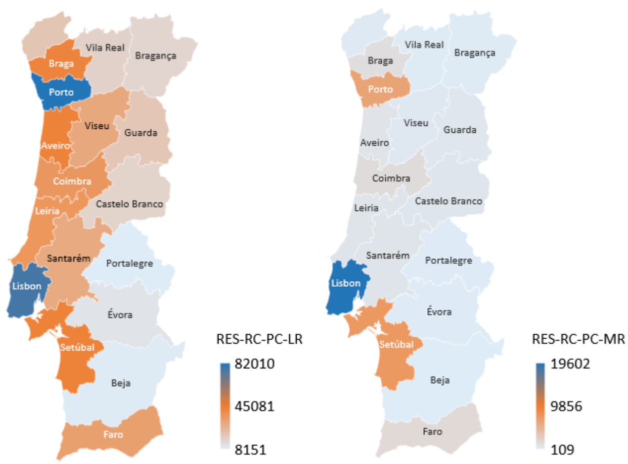

a) b)

Figure 7 Distribution of the residential pre-code RC buildings in mainland Portugal: (a) low-rise; (b) mid-rise

The reconstruction costs per square metre included in the exposure model for structural and non-structural components are provided for rural areas, urban areas, and "big cities" (Porto, Lisbon, and Setubal), according to the census data. The values were obtained from expert sources and then validated and calibrated using the data provided in [24]. The procedure is described in [10]. Those costs are assumed to comprise 80% of the total replacement cost, which also includes that of the buildings' contents. Hence, the total replacement cost is divided as follows: 30% for structural; 50% for non-structural; 20% for contents. Filtering the global data to include just the reconstruction cost of structural components for the two building classes considered in this study (i.e., RES-RC-PC-LR and

RES-RC-PC-MR), the corresponding economic values for each are, respectively, 20 227 M€ and 10 414 M€.

4.3 Vulnerability model

As previously referred, the conversion of fragility functions into vulnerability functions requires the definition of a consequence model that relates each damage state with the expected loss ratio (i.e., ratio of absolute economic loss to total replacement cost). Several proposals are found in the literature for different regions, building typologies, and definitions of damage states (e.g., [25], [26], [27]). The choice of a consequence model has direct impact on the shape of the vulnerability functions, as it defines the contribution of each damage state to the resulting loss ratio per intensity measure level. However, as the fragility functions in this study were derived solely for the LS of SD, the definition of the consequence model came down to defining the loss ratio for a single damage state. As such, based on the characterization given in EC8-3 (2005) for the LS of SD (reproduced in sub-section 3.2 for the reader's convenience), a loss ratio of 80% was considered for the buildings' structural components.

4.4 Risk assessment

The results of the loss assessment process for the above-defined earthquake scenarios are given below in terms of loss ratios, for the original (PC) and retrofitted (R1 and R2) structures, disaggregated by the country's districts. The presented values correspond to the mean loss ratios over those obtained for each of the 1000 generated ground motion fields. The distribution of the RES-RC-PC buildings in mainland Portugal (i.e., the data behind the maps shown in Figure 7) is given in Table 4, along with the corresponding reconstruction cost of their structural components. The obtained structural loss ratios are then given in tables 5 and 6, respectively for the onshore and offshore events (districts with PC loss ratios below 5% were omitted).

Table 4 Distribution and structural value of the residential pre-code RC buildings in mainland Portugal

District	Number of buildings			Structural value (M€)		
	LR	MR	TOTAL	LR	MR	TOTAL
Aveiro	43 328	993	44 321	1289	181	1470
Beja	8709	109	8818	258	20	278
Braga	42 558	1336	43 894	1339	227	1566
Bragança	15 380	267	15 647	424	29	453
Castelo Branco	16 260	760	17 020	488	110	598
Coimbra	36 326	1497	37 823	1098	241	1339
Évora	11 499	189	11 688	363	33	396
Faro	33 415	1688	35 103	1216	395	1611
Guarda	20 450	650	21 100	566	66	632
Leiria	36 751	842	37 593	1140	163	1303
Lisboa	77 196	19 602	96 798	3822	5290	9112
Portalegre	8151	211	8362	239	44	283
Porto	82 010	6398	88 408	3247	1234	4481
Santarém	30 193	861	31 054	925	158	1083
Setúbal	43 419	7437	50 856	1918	2049	3967
Viana do Castelo	20 844	342	21 186	585	54	639
Vila Real	16 736	278	17 014	474	43	517
Viseu	30 554	513	31 067	836	77	913
TOTAL	573 779	43 973	617 752	20 227	10 414	30 641

Table 5 Mean structural loss ratios (%) for the onshore seismic event

District	LR			MR		
	PC	R1	R2	PC	R1	R2
Lisboa	21.2%	28.0%	4.8%	9.3%	22.0%	4.4%
Setúbal	9.2%	11.0%	2.0%	1.6%	4.8%	1.1%

Table 6 Mean structural loss ratios (%) for the offshore seismic event

District	LR			MR		
	PC	R1	PC	R1	PC	R1
Beja	16.0%	12.6%	1.3%	3.2%	6.6%	0.9%
Castelo Branco	5.0%	1.9%	0.1%	0.4%	1.1%	0.1%
Coimbra	5.2%	2.1%	0.1%	0.5%	1.3%	0.1%
Évora	11.2%	6.4%	0.6%	1.6%	4.8%	0.6%
Faro	22.2%	20.4%	2.5%	5.9%	11.7%	2.0%
Leiria	7.7%	3.9%	0.3%	1.1%	2.4%	0.2%
Lisboa	14.0%	9.7%	0.9%	2.5%	6.1%	0.7%
Portalegre	7.4%	3.7%	0.3%	0.6%	2.3%	0.1%
Santarém	8.6%	4.5%	0.3%	1.0%	2.6%	0.2%
Setúbal	16.2%	12.6%	1.3%	3.1%	8.0%	0.9%

4.5 Discussion

The outcomes of the loss assessment process led to different conclusions, depending essentially on the seismic rupture (offshore or onshore), number of storeys (LR or MR), and type of retrofitting system (R1 or R2). For the offshore event, the maximum loss ratios for the PC structures were obtained in the Algarve region and consistently decreased moving North. However, significant differences were found between the results for the LR and MR buildings, with the former varying between 2.5% and 22.2%, and the latter between 0.1% and 5.9%. Given the high magnitude of the offshore event, a mean loss ratio of 5.9% in the Algarve region (for instance) seems relatively low and may eventually be explained (at least in part) by some difficulty in obtaining reliable spectral accelerations for higher periods of vibration when using the GMPE proposed by Akkar and Bommer [9], but this matter will not be further explored herein (the interested reader is referred to [21] for more details on this effect). As for the onshore event, the maximum loss ratios for the PC structures were obtained in the Lisbon district (21.2% and 9.3% for the LR and MR buildings, respectively), followed by the Setúbal district (9.2% and 1.6%), and with all other returning loss ratio values below 1%, regardless of the number of storeys.

Concerning the effect of the retrofitting systems on the loss assessment process, two different situations were identified within the results for the offshore event: (i) for the LR buildings, consistent reductions were observed in the calculated loss ratios, with those for the R2 systems being the most expressive; (ii) for the MR buildings, the R1 systems seem to consistently increase the calculated loss ratios, while the R2 systems cause the expected reduction. What happens with the R1 systems for the MR buildings, although surprising, is most likely related with the above-mentioned limitations concerning the Akkar and Bommer [9] GMPE. Considering the vibration periods' strong reduction caused by the retrofitting systems (thus leading to spectral accelerations which are both higher and more realistic), along with the fact that the fragility curves for the PC-MR structures are relatively close to those of the R1-MR structures (see Figure 4-b), this situation may be explained. As for the onshore event, while the R1 systems seem to be counter-productive for both the LR and the MR buildings, the R2 systems cause a significant reduction of the calculated loss ratios. The fact that spectral accelerations tend to be strongly amplified by the GMPE in the short period range, in locations close to the seismic rupture, might contribute to explain the situation with the R1 systems. Nonetheless, the question remains about the adequateness of the code spectrum used to define the seismic demand for the Lisbon region during the retrofitting design process (it is recalled that the R2 systems were meant essentially for structures in the Faro district).

To illustrate the evolution between the original conditions and those created by the strengthening interventions, loss ratio maps were created for the retrofitted structures and are given below in figures 8 and 9. Being outside the scope of this work, no cost-benefit analysis was carried out to help decide which retrofitting systems should be used (if any). As such, those choices were made imposing a mean loss ratio limit of 5% for the retrofitted structures, being indicated through grey shading above in tables 5 and 6 (readers should note that no retrofitting systems were applied to structures located in districts with PC loss ratios below 5%). The obtained reduction of structural losses is well evident, thus further demonstrating the effectiveness of the retrofitting process based on the design methodology that is proposed in [4].

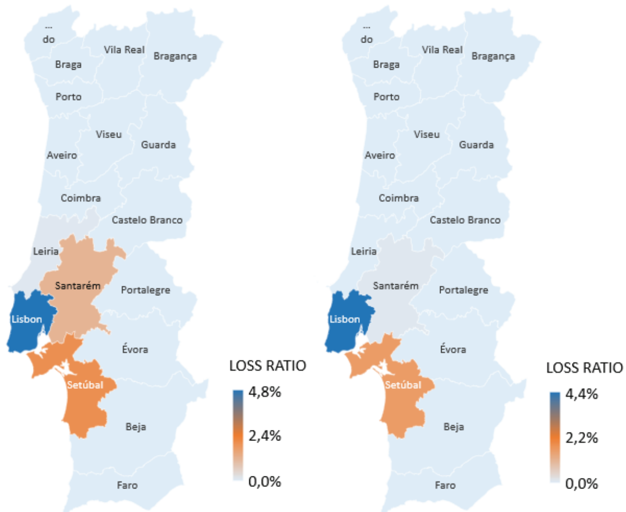

a) b)

Figure 8 Distribution of mean structural loss ratios, after retrofitting, for the onshore seismic event: a) LR; b) MR

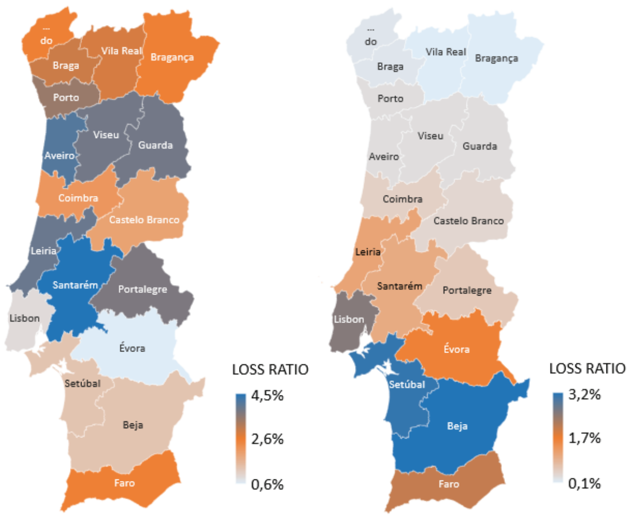

a) b)

Figure 9 Distribution of mean structural loss ratios, after retrofitting, for the offshore seismic event: a) LR; b) MR

5 Concluding remarks

This paper presented a short seismic risk study of a small sample of structures, for the purpose of validating the designed retrofitting systems beyond the requirements of the assessment code. Fragility functions were derived for the before and after retrofitting situations, and the accomplished reduction in the seismic risk to which the structures are exposed was demonstrated through a comparison of loss ratios provided by the *OpenQuake* engine. These conclusions further contribute to validate the design methodology proposed in [4] and demonstrate it is robust enough to be systematically used by practitioners involved in the seismic assessment and retrofitting of existing RC structures. Moreover, other preliminary conclusions were drawn in parallel (for instance, regarding the behaviour of the GMPE), which will surely contribute to improve the preparation of the more complete seismic risk studies to be carried out in the near future.

Acknowledgements due for financial support

– Portuguese Foundation for Science and Technology (FCT) – individual Ph.D. grant (SFRH/BD/103473/2014).
– Project "SMARTER – Seismic urban risk assessment in Iberia and Maghreb" (PT-DZ/0002/2015).
– Project "MitRisk – Framework for seismic risk reduction resorting to cost-effective retrofitting solutions" (PTDC/ECI--EST/31865/2017 – POCI/01/0145/FEDER/031865, funded by FEDER funds through COMPETE2020 – *Programa Operacional Competitividade e Internacionalização* (POCI), and by national funds (PIDDAC) through FCT/MCTES).
– Base Funding – UIDB/04708/2020 and Programmatic Funding – UIDP/04708/2020 of the CONSTRUCT – *Instituto de I&D em Estruturas e Construções* – funded by national funds through the FCT/MCTES (PIDDAC).

References

[1] Rossetto, T.; Elnashai, A. (2005 – "A new analytical procedure for the derivation of displacement-based vulnerability curves for populations of RC structures". *Engineering Structures*, 27 (3): 397-409.

[2] Silva, V.; Crowley, H.; Varum, H.; Pinho, R.; Sousa, R. (2014) – "Evaluation of analytical methodologies used to derive vulnerability functions". Earthquake *Engineering* & *Structural Dynamics*, 43 (2): 181-204.

[3] Silva, V.; Crowley, H.; Pagani, M.; Monelli, D.; Pinho, R. (2014) – "Development of the *OpenQuake* engine, the Global Earthquake Model's open-source software for seismic risk assessment". *Natural Hazards*, 72 (3): 1409-1427.

[4] Falcão Moreira, R. (2022) – "Seismic risk reduction of reinforced concrete buildings retrofitted with steel braces". Ph.D. thesis. University of Porto, Porto, Portugal.

[5] Silva, V. (2013) – "Development of open models and tools for seismic risk assessment: application to Portugal". Ph.D. thesis. University of Aveiro, Aveiro, Portugal.

[6] Bommer, J.J.; Spence, R.; Erdik, M.; Tabuchi, S.; Aydinoglu, N.; Booth, E.; Re, D.D.; Pterken, D. (2002) – "Development of an earthquake loss model for Turkish catastrophe insurance". *Journal of Seismology*, 6: 431-446.

[7] Carvalho, A.; Zonno, G.; Franceschina. G.; Bilé Serra, J.; Campos Costa, A. (2008) – "Earthquake shaking scenarios for the metropolitan area of Lisbon". *Soil Dynamics and Earthquake Engineering*, 28 (5): 347-364.

[8] Atkinson, G.M.; Boore, D.M. (2006) – "Earthquake ground motion prediction equations for eastern North America". *Bulletin of the Seismological Society of America*, 96 (6): 2181-2205.

[9] Akkar, S.; Bommer, J. (2010) – "Empirical equations for the prediction of PGA, PGV, and spectral accelerations in Europe, the Mediterranean region, and the Middle East". *Seismological Research Letters*, 81 (2): 195-206.

[10] Crowley, H.; Dabbeek, J.; Despotaki, V.; Rodrigues, D.; Martins, L.; Silva, V.; Romão, X.; Pereira, N.; Weatherill, G.; Danciu, L. (2021) – *European Seismic Risk Model (ESRM20)*. EFEHR Technical Report 002 V1.0.0, https://doi.org/10.7414/EUC-EFEHR-TR002-ESRM20.

[11] Macedo, L. (2017) – "Performance-based seismic design and assessment of steel moment frame buildings". Ph.D. thesis. University of Porto, Porto, Portugal.

[12] Araújo, M.; Macedo, L.; Marques, M.; Castro, J.M. (2016) – "Code--based record selection methods for seismic performance assessment of buildings". *Earthquake Engineering* & *Structural Dynamics*, 45: 129-148.

[13] Macedo, L.; Castro, J.M. (2017) – "SelEQ: An advanced ground motion record selection and scaling framework". *Advances in Engineering Software*, 114: 32-47.

[14] Akkar, S.; Sucuoglu, H.; Yakut, A. (2005) – "Displacement-based fragility functions for low- and mid-rise ordinary concrete buildings". *Earthquake Spectra*, 21 (4): 901-927.

[15] Priestley, M.J.N. (1998) – "Displacement-based approaches to rational limit states design of new structures". *Proceedings of the 11th European Conference on Earthquake Engineering*. Rotterdam, The Netherlands.

[16] Ghobarah, A. (2004) – "On drift limits associated with different damage levels". *Proceedings of International Workshop on Performance-Based Seismic Design*. Bled, Slovenia.

[17] Sassun, K.; Sullivan, T.J.; Morandi, P.; Cardone, D. (2015) – "Characterizing the in-plane seismic performance of infill masonry". *Bulletin of the New Zealand Society for Earthquake Engineering*, 49 (1): 100-117.

[18] Sousa, R.; Batalha, N.; Silva, V.; Rodrigues, H. (2021) – "Seismic fragility functions for Portuguese RC precast buildings". *Bulletin of Earthquake Engineering*, 19: 6573-6590.

[19] Moreira, V. (1989) – "Seismicity of the Portuguese continental margin". In S. Gregersen, P.W. Basham (Eds.), Earthquakes at North-Atlantic Passive Margins: Neotectonics and Postglacial Rebound. Chapter 31: 533-545. Kluwer Academic Publishers. ISBN 978-94-010-7538-1.

[20] Silva, V.; Marques, M.; Castro, J.M.; Varum, H. (2015) – "Development and application of a real-time loss estimation framework for Portugal". *Bulletin of Earthquake Engineering*, 13 (9): 2493-2516.

[21] Vilanova, S.; Fonseca, J.; Oliveira, C. (2012) – "Ground motion models for seismic hazard assessment in Western Iberia: Constraints from instrumental data and intensity observations". *Bulletin of the Seismological Society of America*, 102 (1): 169-184.

[22] Silva, V.; Crowley, H.; Varum, H.; Pinho, R. (2015) – "Seismic risk assessment for mainland Portugal". *Bulletin of Earthquake Engineering*, 13 (2): 429-457.

[23] RSA (1983) – *Regulamento de Segurança e Acções para Estruturas de Edifícios e Pontes*. Lisbon, Portugal: Decreto-Lei n.º 235/83 (in Portuguese).

[24] Paprotny, D.; Kreibich, H.; Morales-Nápoles, O.; Terefenko, P.; Schröter, K. (2020) – "Estimating exposure of residential assets to natural hazards in Europe using open data". *Natural Hazards and Earth Systems Science*, 20: 323-343.

[25] Di Pasquale, G.; Goretti, A. (2001) – "Vulnerabilità funzionale ed economica degli edifici residenziali colpiti dai recenti eventi sismici italiani". *Proceedings of the 10th National Conference "L'Ingegneria Sismica in Italia"*. Potenza-Matera, Italy.

[26] Kappos, A.J.; Panagopoulos, G.; Panagiotopoulos, C.; Penelis, G. (2006) – "A hybrid method for the vulnerability assessment of RC and URM buildings". *Bulletin of Earthquake Engineering*, 4 (4): 391-413.

[27] Bal, I.; Crowley, H.; Pinho, R.; Gulay, F. (2008) – "Detailed assessment of structural characteristics of Turkish RC building stock for loss assessment models". *Soil Dynamics and Earthquake Engineering*, 28 (10-11): 914-932.